

Presented at the International Symposium  
on Aero-Space Nuclear Propulsion,  
Las Vegas, Nevada, October, 1961

EXPERIMENTAL RESULTS OF RAPID IN-CORE FLUX MAPPING TECHNIQUES  
IN THE PLUM BROOK REACTOR

R. Steinberg  
National Aeronautics and Space Administration  
Lewis Research Center  
Cleveland, Ohio

Summary

The problems associated with flux mapping in the Plum Brook Research Reactor, which employs an 18 plate Materials Testing Reactor type fuel element, are discussed fully. Design of a flux survey instrument is presented which, utilizing four solid state fission probes, makes it possible to map the complete Plum Brook core in a little over 6 hours, with the data presented in a form immediately available for analysis. Mapping a fuel element (from even 30 ft. above the core) does not require an accurate above water positioning system, yet a high degree of accuracy ( $\pm 0.1$  in.) in referencing in-core measurements has been obtained.

The effect of radiation on the semiconductor detectors and the operating characteristics of the instrument, along with typical flux profiles obtained in mapping the Plum Brook Reactor are presented.

Introduction

One June 14, 1961, the National Aeronautics and Space Administration's Plum Brook Research Reactor (PBR) went critical. In anticipation of the many flux measurements which would be required in the power reactor and its low power mock-up (MUR)

(THRU)  
None  
(CODE)  
(CATEGORY)

N65-86903  
(ACCESSION NUMBER)  
29  
(PAGES)  
TMA-56685  
(NASA CR OR TMX OR AD NUMBER)

FACILITY FORM 602

E-1486

Godard

a program was initiated to look into ways and means of reducing the time required for flux mapping and to increase the accuracy of the measurement.

The PBR is a high flux, heterogeneous, enriched fuel, thermal reactor employing an 18 plate Materials Testing Reactor (MTR) type fuel element (see fig. 1) in a 3 by 9 array. The standard approach to mapping a core of this type has been to irradiate wires or foils suspended in the water channels between the closely spaced (0.110 in.) fuel plates. After removal of the wires from the core, the flux at each point is then determined from the measured activity along the length of the wire. The fact that measurements by means of induced activity require two steps, i.e., the irradiation followed by the activity measurements, makes this technique quite lengthy and involved.

Using an ionization chamber combines the irradiation and the measurement into an instantaneous indication of the neutron flux. While most ionization chambers are rather large, recent advances in semiconductor technology have made possible extremely small solid state fission detectors.

The purpose of this paper is (1) to describe an instrument<sup>1</sup> which, utilizing semiconductor detectors, can be used for rapid and accurate low power flux mapping in reactors employing MTR type fuel elements and (2) to present experimental results obtained in mapping the PBR.

### Design Aspects of Instrument

The problem of obtaining the flux distribution in a plate type fuel element is essentially two-fold; first, a detector must be made small enough to pass between the closely spaced fuel plates, and second, a means must be provided to position the detector easily and to record exactly where the measurement is made. The difficulties of positioning through 10 ft. of shielding (see fig. 2) water are compounded by the core structural material and the control rod guide bearing supports, which partly obscure the fuel elements.

The flux survey instrument utilizes four solid state fission probes, which are simultaneously driven between fuel plates. Each probe is 50 in. long, with a rectangular cross section of 0.092 by 0.28 in. (see fig. 3). The probe housing is constructed of aluminum, and the two signal leads running the length of the probe including the detector are potted in paraffin. Removable tips are provided for detector replacement. A set of four detectors can be changed in about 1/2 hour.

The instrument as shown in figure 4 is 60 in. long and 2.75 in. in diameter. The probe guide has a special head, which contains a microswitch-actuated circuit, which establishes the necessary x-y coordinate system and allows the instrument to be positioned from above on its own supporting cable. The leading surface of the guide pins has a narrow groove (into which the microswitch-actuator is extended) traversing its length, and two nylon guide located on a line perpendicular to the direction of the groove.

The probe guide head, made of red Lucite so as to be visible under water, is shaped to pass into the upper fuel element end box with a minimum of clearance.

All four probes are mounted on a watertight Lucite carriage, which rides on an aluminum drive screw and two stainless-steel guide rods. A pulley mechanism is used to take up the slack in the four coaxial signal cables as the probes are driven down between fuel plates. This removes the possibility of the signal cables becoming entangled in the control rod mechanisms. The pulley arrangement is accomplished by allowing the signal cables, which enter the Lucite carriage through the probe housings, to reverse direction and leave through watertight fittings in the carriage. The coaxial signal cables again reverse direction by passing around a weighted pulley and continue on up through a passage in the center of the Lucite carriage. A clamp arrangement is provided just under and on the side of the motor housing to hold the signal cable securely in place.

The uppermost portion of the instrument contains the drive motor with its associated clutch mechanism and a potentiometer coupled to the drive screw. The clutch is provided in case of misalignment; and the potentiometer, in conjunction with a digital voltmeter, serves to record the position (with an accuracy of  $\pm 0.1$  in.) of the detector within the fuel element. A vertical position indicator (shown in fig. 5) consisting of an air bubble in an opaque liquid is attached to the motor housing to facilitate positioning of the instrument. The opaque fluid is contained between two Lucite lenses. A light source, in parallel with the microswitch circuit in the probe



guide head, behind the lenses makes the bubble easily visible through the 10 ft. of shielding water and also serves to indicate when the instrument is correctly seated in the fuel element. The central section of the instrument is housed in a Lucite tube that both protects the four fission probes and adds rigidity to the carriage guides and drive screw. Only the motor housing and the Lucite carriage are watertight; the rest of the instrument is allowed to fill with water. A limiting microswitch at each end of travel automatically reverses the direction of motion of the probes. The four signal leads are brought out of the side of the instrument, while the direct current supply for the drive motor, spacer comb indicator, microswitch reversing circuit, vertical position indicator, and position readout is carried by the main power cable.

#### Underwater Positioning System

The instrument is lowered through the water on its own supporting power cable; the probe guide passes into the fuel element end box and comes to rest atop the fuel plates. Because of the close fit between the probe guide and the fuel element end box, only one of three possible alternatives can occur:

(1) The spacer comb of the fuel element has not quite entered the grooved probe guide head, in which case the microswitch circuit has not been actuated.

(2) The spacer comb has entered the grooved probe guide head allowing the nylon guide pins to come to rest atop a fuel plate, in which case the microswitch circuit will not be actuated.

(3) The spacer comb has entered the grooved probe guide head allowing the nylon pins to come to rest between fuel plates, actuating the microswitch circuit which indicates that the instrument is in operating position (see fig. 6).

The fact that the microswitch circuit has been actuated is indicated by a light on the control console and in the vertical position indicator. The light in the indicator illuminates both the air bubble and the rim of the unit for ease of centering the bubble. An accurate vertical reference not only makes possible rapid positioning of the instrument on the fuel element (1 min is normal), it also insures repeatability in positioning the fission probes since the instrument can be aligned to within 1 degree of the vertical. A positive indication of the spacer comb actuated signal light always means that the instrument must be in the correct operating position since the microswitch cannot be actuated unless the nylon guide pins are between fuel plates. As an additional safety factor the drive motor will not operate unless the comb light circuit has been actuated. The PBR fuel element has a spacer comb at both ends of the fuel plates. Experience has shown that it is possible to hit the bottom spacer comb with two of the four probes. When this occurs (introduction of the vertical position indicator has all but eliminated this problem) the instrument raises up off the fuel element. Because of the motor override control in the spacer comb circuit, after the instrument has moved up 0.1 in. the motor voltage is cut off.

Although the mapping was done through 10 ft. of shielding water, the instrument has been satisfactorily positioned in a fuel element from 30 ft. above the core.

### Solid State Detectors

A solid-state fission probe can be likened to a gaseous ionization chamber, in that the voltage pulse produced per incident ionizing particle depends upon the collection of electron-hole (e-h) pairs which are formed by the passage of the ionizing radiation. The semiconductor detecting element consists of a single silicon p-n junction wafer coated with uranium-235. A voltage pulse, produced by a neutron induced fission fragment, results from the collection of e-h pairs in the region of the p-n junction. While some recombination and trapping will occur a large number of the e-h pairs will travel to within a diffusion length of the p-n junction and be separated by the field within the junction. The pulse thus produced is proportional to the particle energy divided by the junction capacitance and the ionization potential of silicon.

### Operational Characteristics

Each detector has a thermal neutron sensitivity of  $\sim 2.5 \times 10^{-4}$  counts/n/cm<sup>2</sup>. In figure 7 is shown a typical response curve which demonstrates the ability of the detector to discriminate between fission fragments and alpha decay and background noise. At the low power level at which the flux mapping was done, there have been no observable effects from gamma radiation. This is reasonable since a gamma ray provides such a low ionization density that only a small fraction of its energy is dissipated within the range of the junction. As a result, pulse height discrimination against gamma fluxes is complete except for pile-up encountered in extremely high fluxes.

The total worth ( $\Delta k/k_{\text{eff}}$ ) of all four probes when fully inserted in the core is less than 0.00015. Correcting for this small flux perturbation and maintaining constant power, as can be seen from figure 8, which shows a plot of reactor power during the mapping of element LD-6, presents no problem.

The time involved in making a single traverse is determined by the desired accuracy in counting and spatial resolution. The first complete mapping of the PBR was done at a power level of 2 watts to obtain a maximum count rate of 10,000 counts/sec and a spatial resolution of 0.5 in. Two hundred and forty measurements per element were made, making a total of over 5000 data points for the complete core. While a 0.5 in. resolution was desirable from the standpoint of showing the effect of the water gap in the fuel shims and the peaking in the reflector just below the fuel plates, it was felt that the number of measurements made could be substantially reduced. In a recent mapping of a partially poisoned core, the reactor was run at a power level of 2 watts to obtain 10,000 counts/sec, however, a count was taken over a 2-sec interval; although the spatial resolution was 1 in., the detector's being only 0.375 in. in length meant an increase in resolution could easily be obtained by simply changing the motor speed while the probes are passing through the region of interest. For the poisoned case, a total of 13 elements were mapped in 3 1/2 hours. This includes 6 min to drive the fission probes down between the fuel plates, 6 min to withdraw the probes (measurements were made only during this part of cycle) and 3 min to place the instrument into a new fuel element. In order to gain access to the elements in the LC row (between control rods), an alternate probe guide head was required, which took an additional 15 min to install.

### Radiation Damage

In figure 9 is shown the response of a silicon detector to uranium-235 fission fragments as a function of the integrated thermal flux. The fact that a characteristic fission fragment spectrum is obtained even through there are particles incident at various angles indicates the absence of any substantial dead layer. A rapid reduction in the high energy peak occurs when the carriers, in increasing numbers, recombine before they can diffuse to the junction region. In using the silicon diode as a fission detector, the amplifier discriminator is set just above the noise level. Any subsequent shift in the high energy pulse height will not immediately affect the count rate; however, as can be seen from figure 10, there is an eventual decrease in count rate with irradiation. Three detectors, each coated with a different amount of uranium-235, were irradiated. Since each detector saw substantially the same radiation environment, the observed drop in count rate was probably the result of fission fragment damage. Mapping the PBR at an average count rate of 10,000 counts per measurement and a spatial resolution of 1 in. requires an integrated thermal flux of  $3.4 \times 10^{11}$  NVT to complete all 22 fuel elements. Although it can be seen from figure 10 that at  $3.4 \times 10^{11}$  NVT no significant change in the count rate has occurred, it has been a practice to make a repeat run on the first element mapped every ten elements to detect any shift in count rate. Figure 11 shows a recent mapping of element LB-7 (probe No. 2 position) and a repeat run in the element after ten elements had been mapped. The decrease in the average flux over the element was 0.5%. The fact that the repeat came close is indicative not only of the relatively small amount of damage done,

but also of the ability to place the probe in exactly the same position as the initial run. Since the probes are also equipped with removable tips, for rapidly changing detectors, radiation damage never becomes a problem.

### Control Instrumentation and Data Processing

Figure 12 shows a block diagram of the control instrumentation and readout equipment as well as the circuitry contained within the instrument. Using a charge sensitive preamplifier virtually eliminates the capacitance problem (pulse height inversely proportional to capacitance) and allows 40 ft. of cable between the detector and the preamplifier. A single counting channel is utilized in conjunction with a solenoid actuated coaxial switch, which cycles between probes. The fission pulses are monitored on an oscilloscope, and a dual preset counter controls the counting channel. The data are immediately printed on paper tape, recording the probe number, position in the fuel element and count rate. An x-y point plotter in conjunction with the printer has been provided to afford a visual account of the flux variation within a fuel element and to make the data immediately available for analysis upon completion of the traverse. A typical family of curves made by the plotter during a traverse is shown in figure 13. The complete system is contained within a double rack which during operation is placed within several feet of the pressure vessel. An additional modification is planned which will allow the information simultaneously to be put on IBM cards. This addition will afford an easy way of applying any correction factors and generating average flux values.

### Results of Flux Mapping in PBR

The mapping of the PBR with the survey instrument was done in a cold clean core with the reactor critical on five fuel shims as a bank at 15.4 in. with the three beryllium shims and the two regulating rods fully withdrawn. Figure 14 shows a plan view of the PBR with an insert showing the position of each of the four probes. With the reactor at a power level of 2 watts, measurements were made at 0.5 in. intervals while the probes were in motion. A total of 26 fuel elements were surveyed (including four repeat runs).

Figure 15 shows a family of vertical flux traverses made with probe No. 1 in elements LB-2, LB-3, LB-4, LB-5, and LB-6. The large effect of the fuel shims can be seen from the fact that a major portion of the thermal neutrons and hence the power is generated in the lower half of the element. It is this source of fast neutrons which results in a rather large peaking in the water region below the fuel plates, while the absence of any substantial flux generation at the top of the fuel element causes only a minor peaking in the water region. The local effects of the fuel shims can be seen in the even numbered elements.

The Plum Brook Reactor like the MTR<sup>2</sup> is a heterogeneous reactor, and anything approaching symmetry in a flux distribution (especially for the cold clean condition) is hard to detect. About the only region in which the flux resembles a cosine distribution is a horizontal plane cutting through the flattened portion of the peak thermal flux. Figure 16 shows just such a flux distribution constructed across the LB row at 18.7 in. Probe No. 3 showed a pronounced dip in the flux in the section of element LB-5 closest to the reflector. A check of the vertical traverse

made with probe No. 3 in LB-5 indicated that the flux was low all along the fuel element. The presence of a strong absorber in only one section of LB-5 could very possibly be brazing flux which was not completely removed from the element.

To obtain a more complete understanding of the spatial variation of the thermal flux within the PBR, the average flux of each vertical traverse in the LB row was used to generate a three-dimensional flux distribution (see fig. 17). While the local perturbation in the LB-5 position was expected, the appearance of a hump in the flux close to the beryllium reflector was not immediately understood. In order to take a closer look at the flux near the core reflector interface, a family of horizontal traverses were constructed across elements LB-5, LC-5, LD-5 and also LB-7, LC-7, LD-7 (see fig. 18). The flux in the rod region follows a predictable pattern; however, below the rods the flux profile changes rather rapidly, giving rise to the observed hump. Figure 19 shows a similar family of curves generated across elements LB-3, LC-3, LD-3 and also LB-9, LC-9, LD-9; the same pattern is apparent. In all probability, the local effects of the rods plus the 2 in. water gap in the fuel shims, and the presence of the fuel shims partially extended into the bottom reflector combine to produce the observed irregularities in the flux.

#### Summary of Results

The basic idea behind the instrument was to develop a fast and accurate technique for surveying the flux in the PBR and its low power mock-up. This meant elimination of any complicated above water positioning system while maintaining a high degree of accuracy in referencing the



measurements. The main concern was ease and speed of positioning an instrument which would function perfectly in a water environment. Results of the flux mapping have demonstrated that the instrument has met all design criteria.

#### Acknowledgements

The author wishes to express his appreciation to W. B. Schwab whose technical know-how helped translate the idea into a working model, and for the many invaluable suggestions he made. H. W. Geisler and the Reactor Physics Section at Plum Brook were especially helpful in setting up the apparatus and during the mapping. The author is also indebted to T. A. Fox and the Experimental Reactor Physics Section which aided immeasurably with the initial measurements made with the semiconductor detectors.

#### References

1. Steinberg, R. "Rapid Flux Mapping in MTR Type Fuel Elements,"  
Nucleonics 19, No. 4, April (1961).
2. Bright, G. O., and Shroeder F., "Neutron Flux Distributions in the  
Materials Testing Reactor," IDO-15047, Part I, February (1953).

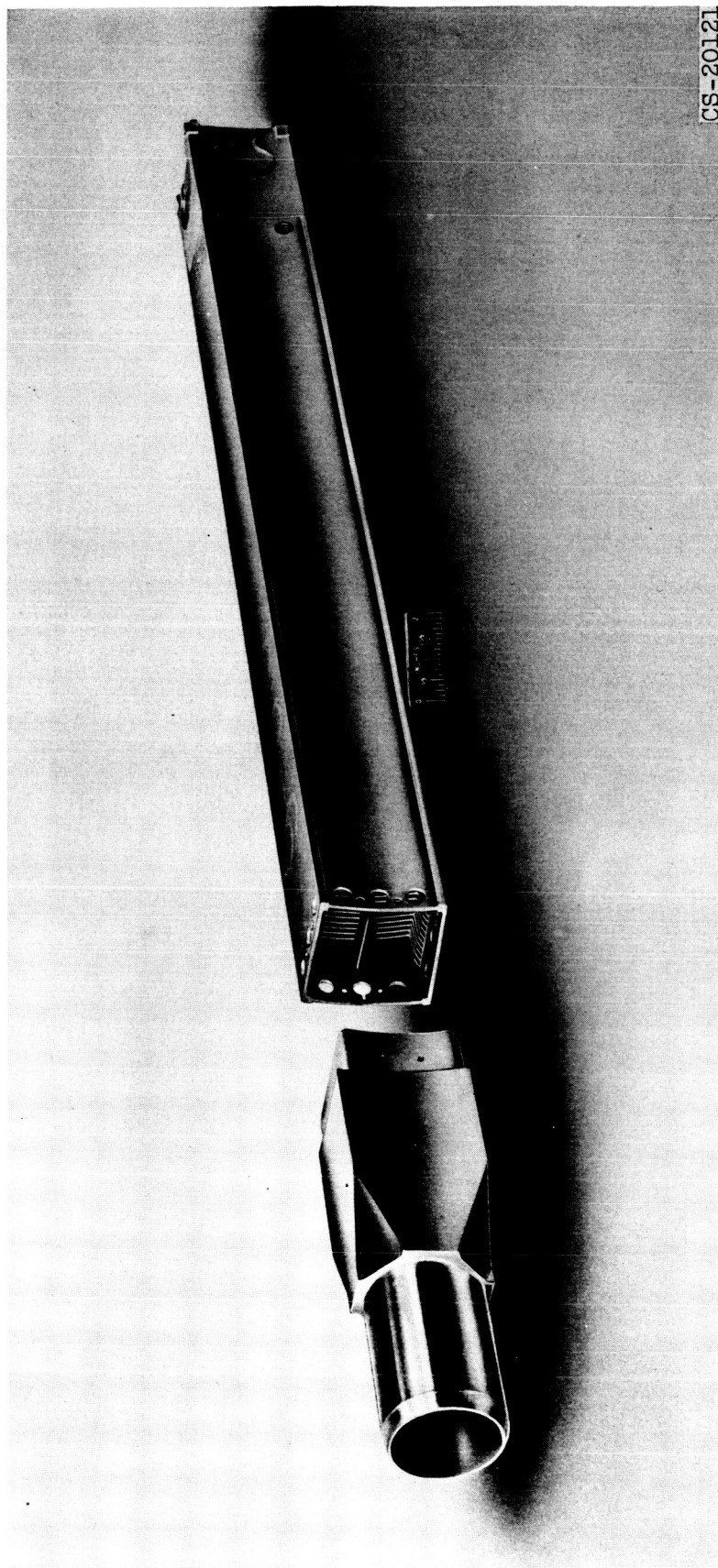


Figure 1. - Eighteen plate PBR fuel element with lower end box removed.

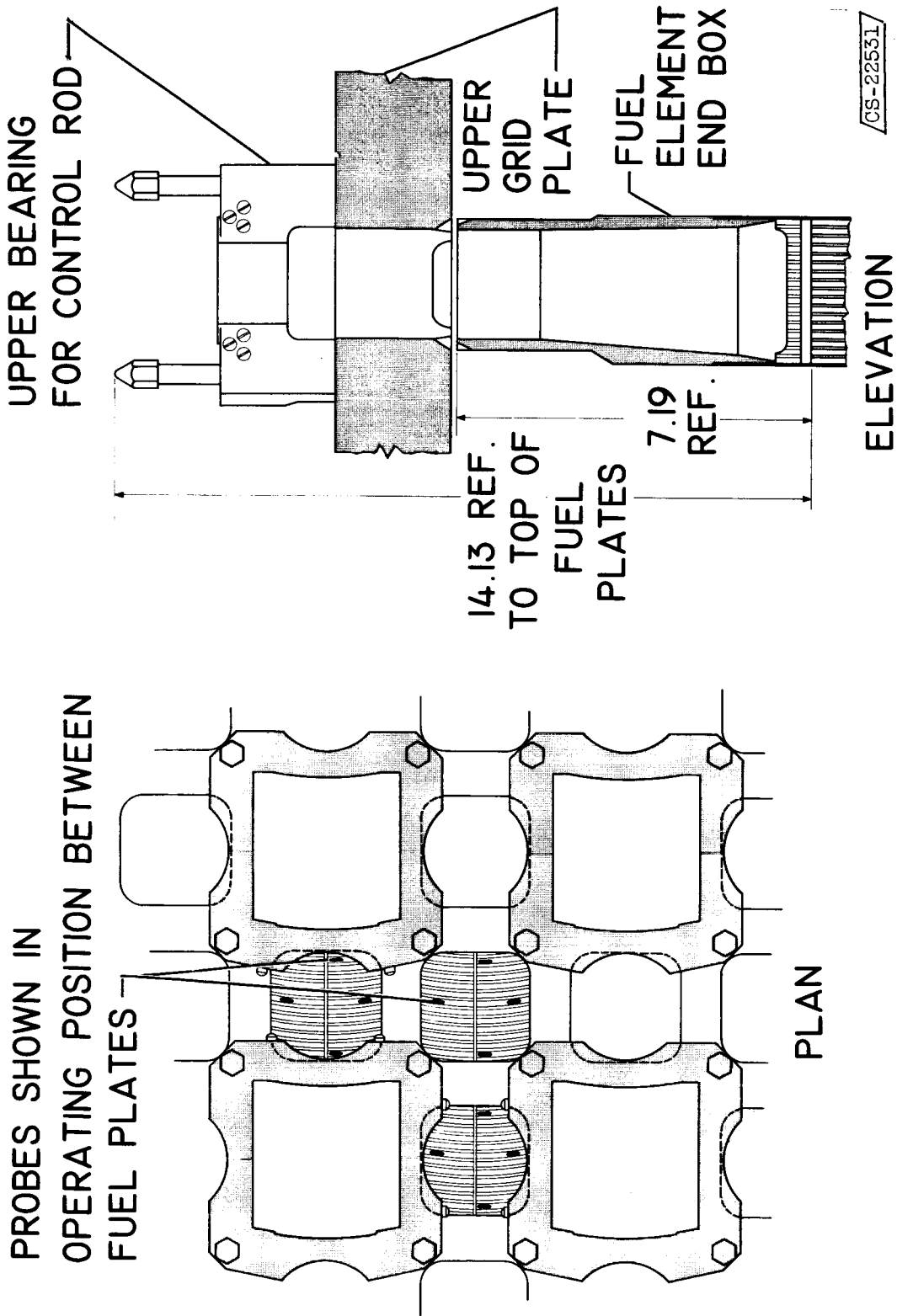
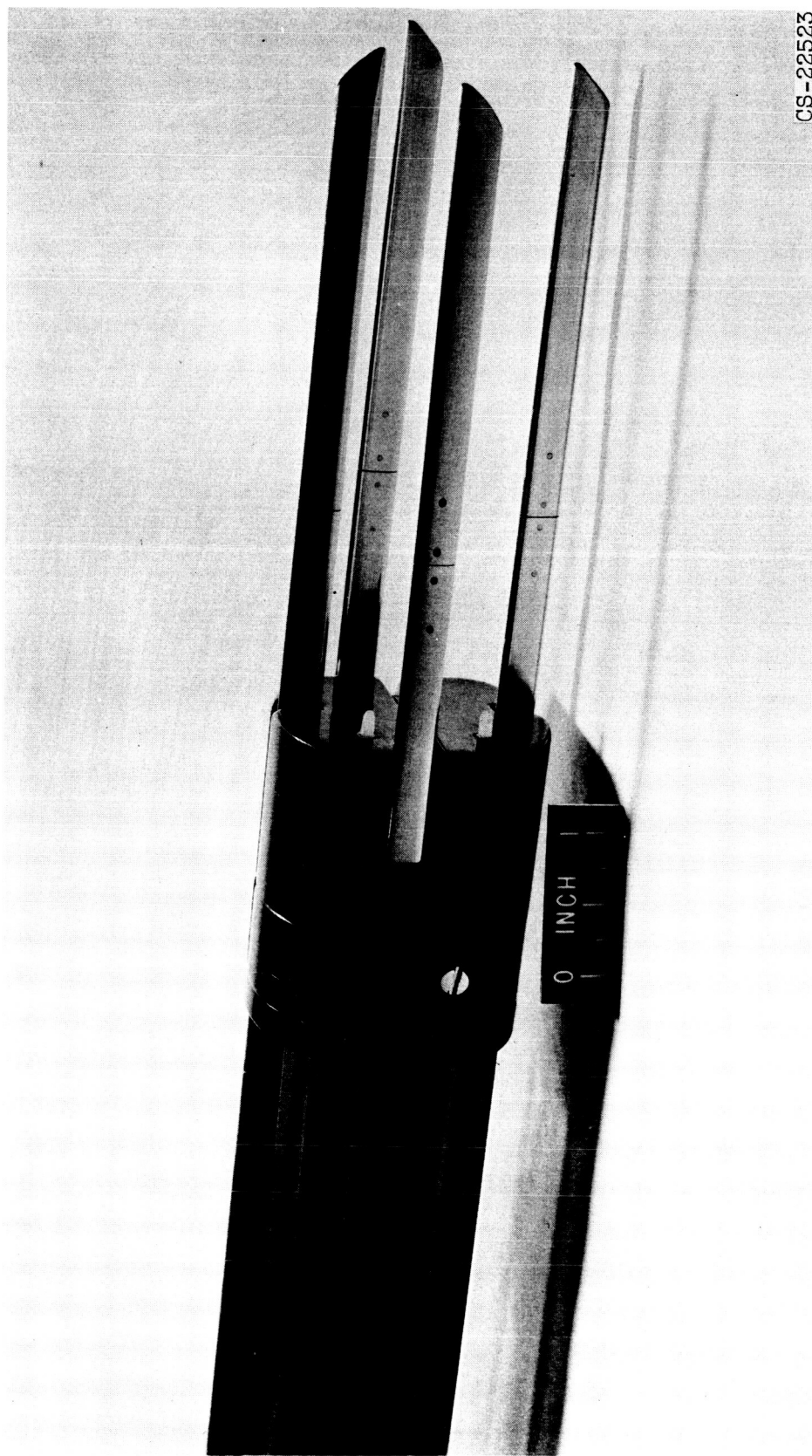


Figure 2. - Section of core showing limited access to fuel elements.



CS-22523

Figure 3. - Probe guide head with probes partially extended showing removable tips.

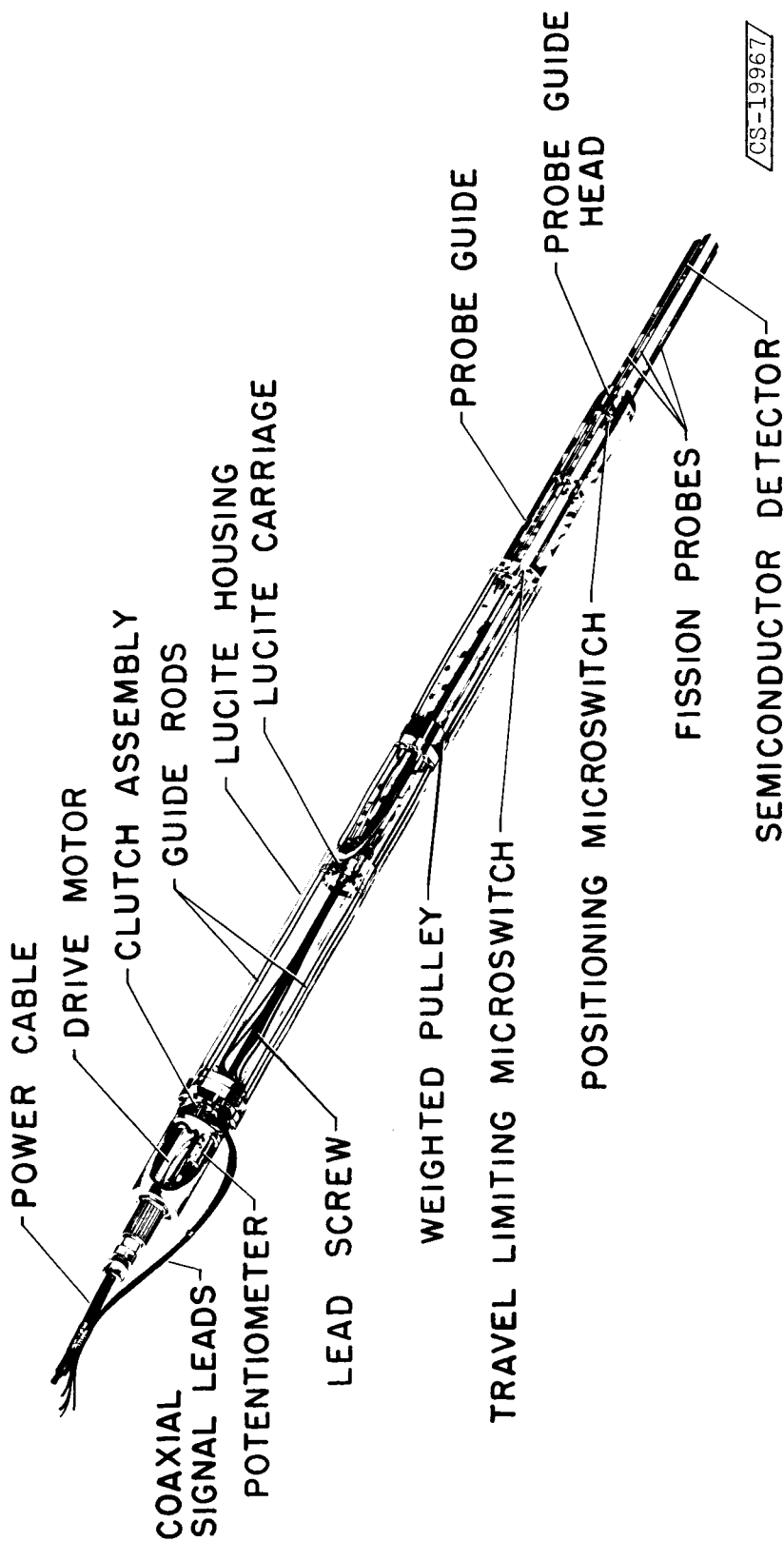
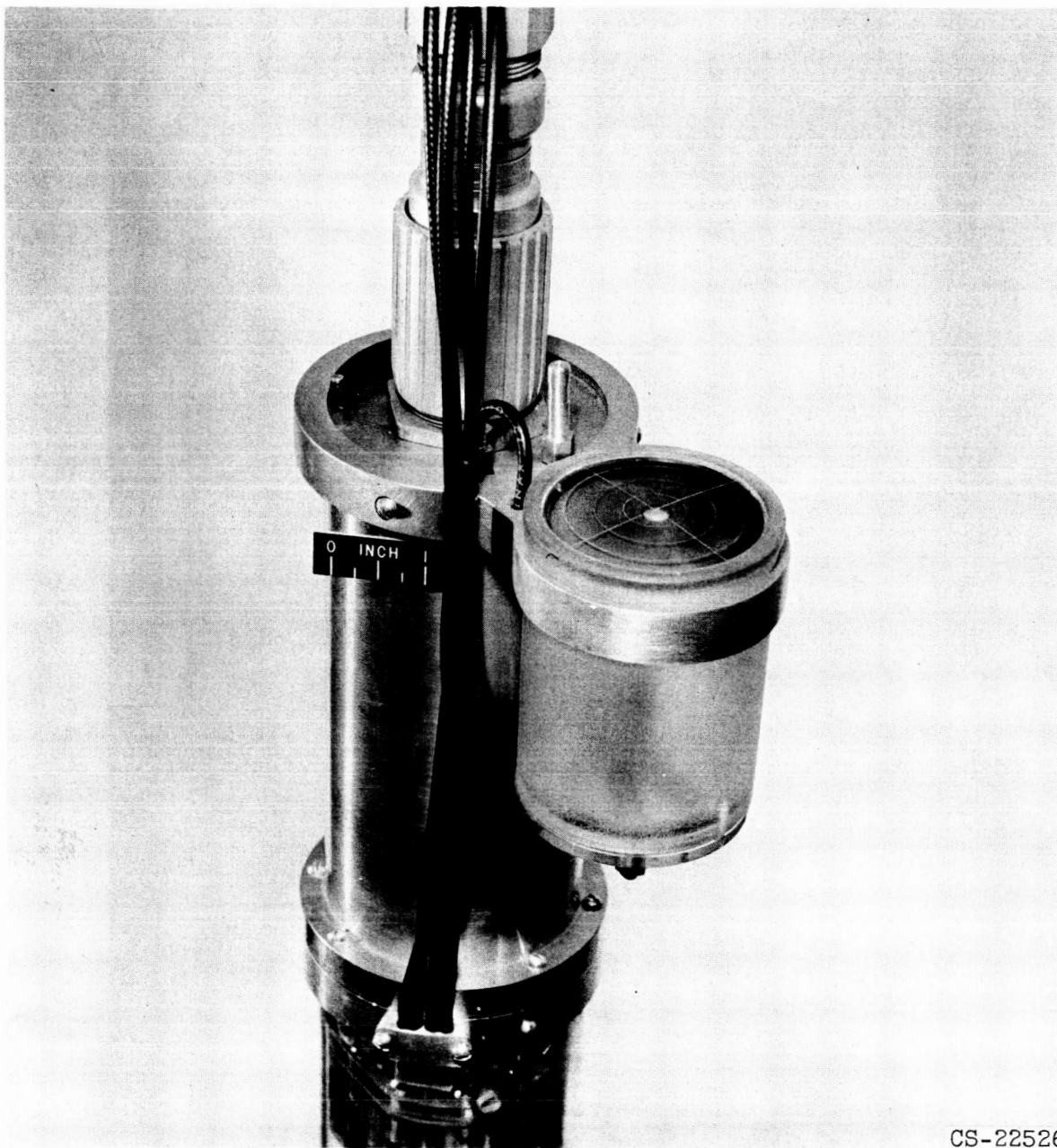
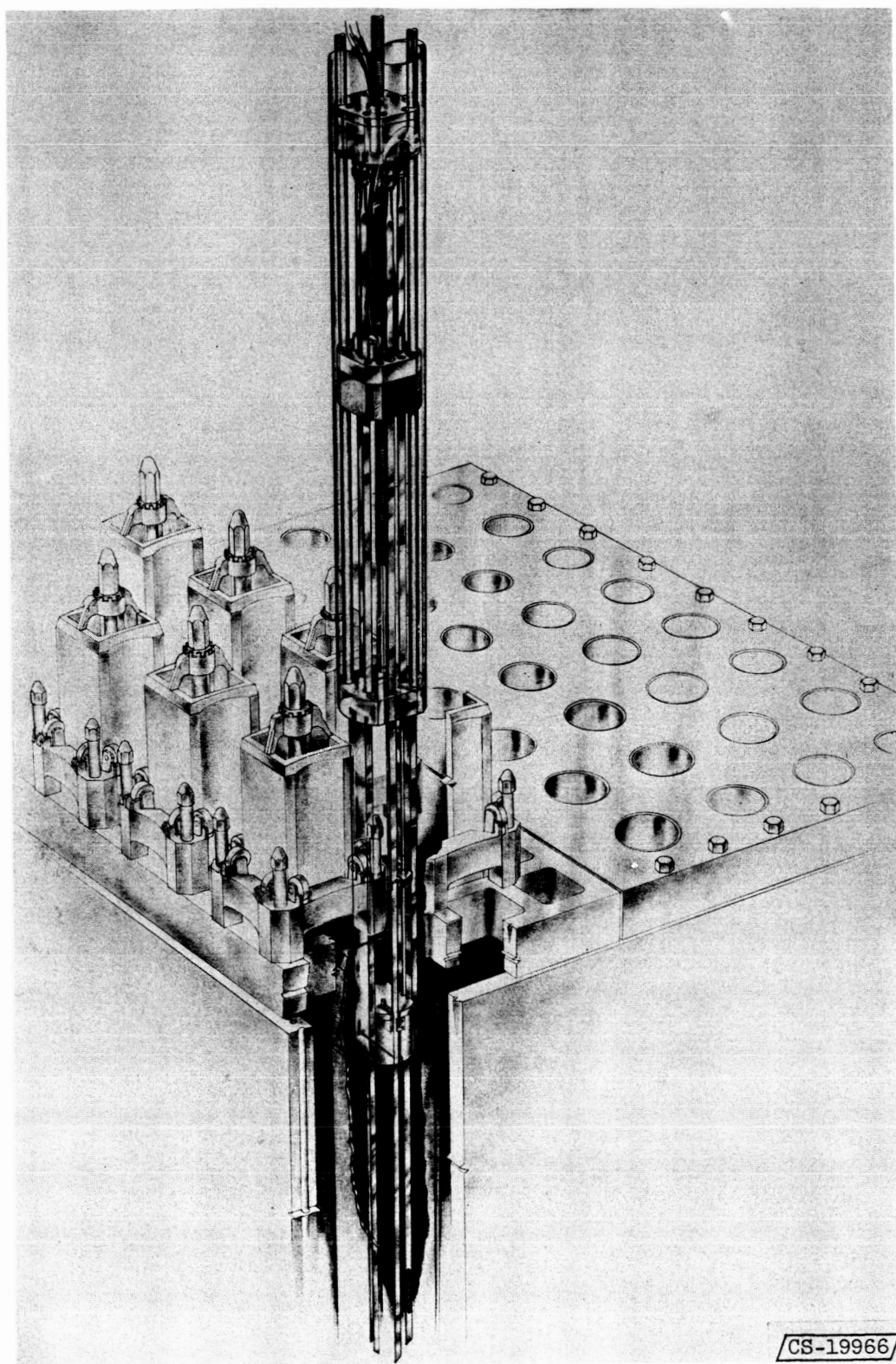


Figure 4. - Flux survey instrument.



CS-22526

Figure 5. - Vertical position indicator mounted on motor housing.



CS-19966

Figure 6. - Instrument in operating position.



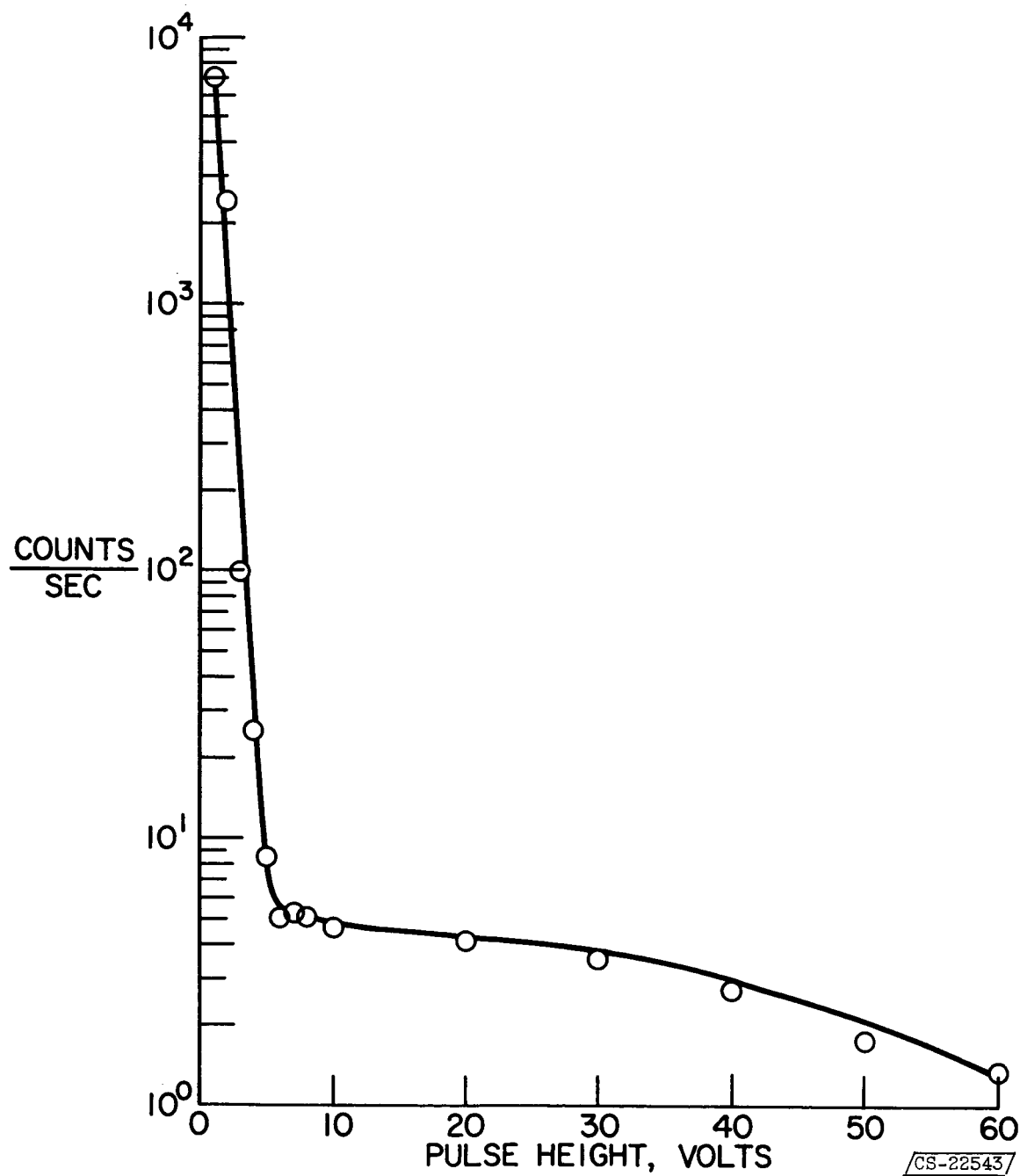


Figure 7. - Typical detector response curve.



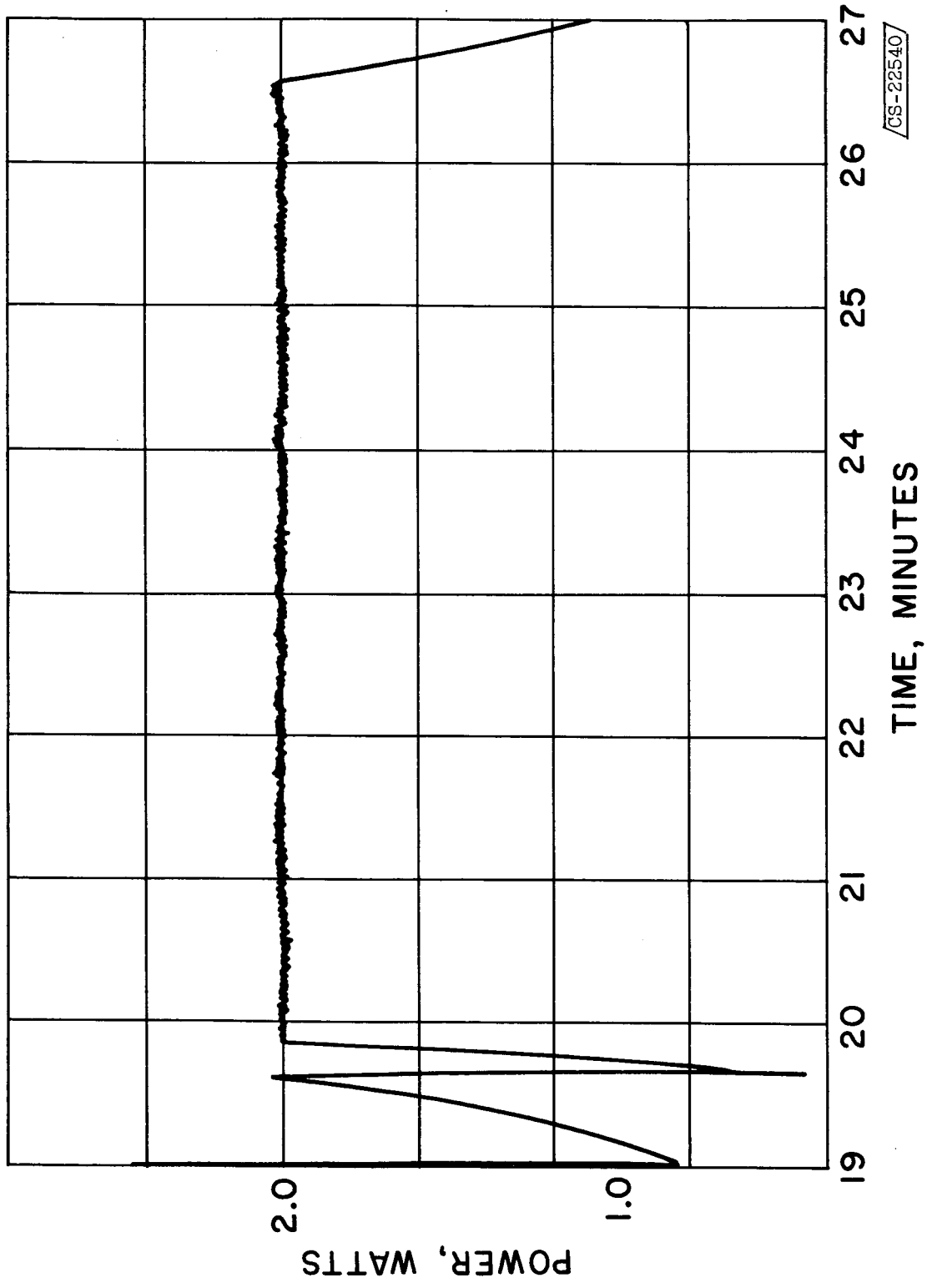


Figure 8. - Reactor power as a function of time during mapping in LD-6 position.

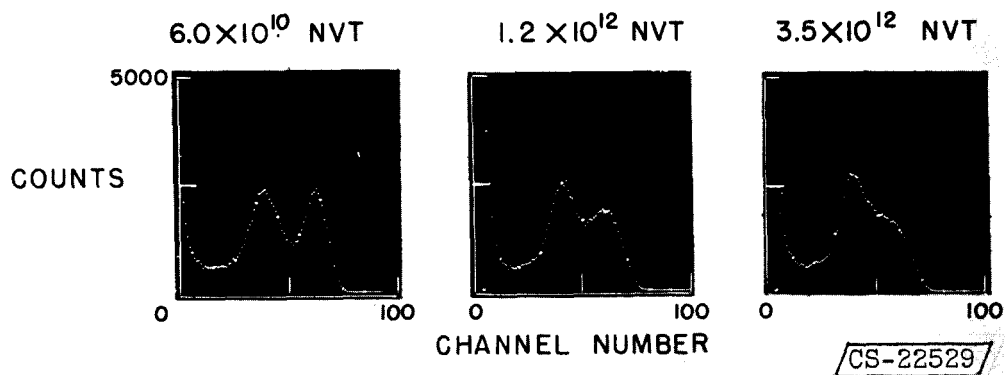


Figure 9. - Response of a silicon detector to uranium-235 fission fragments as a function of integrated thermal flux.

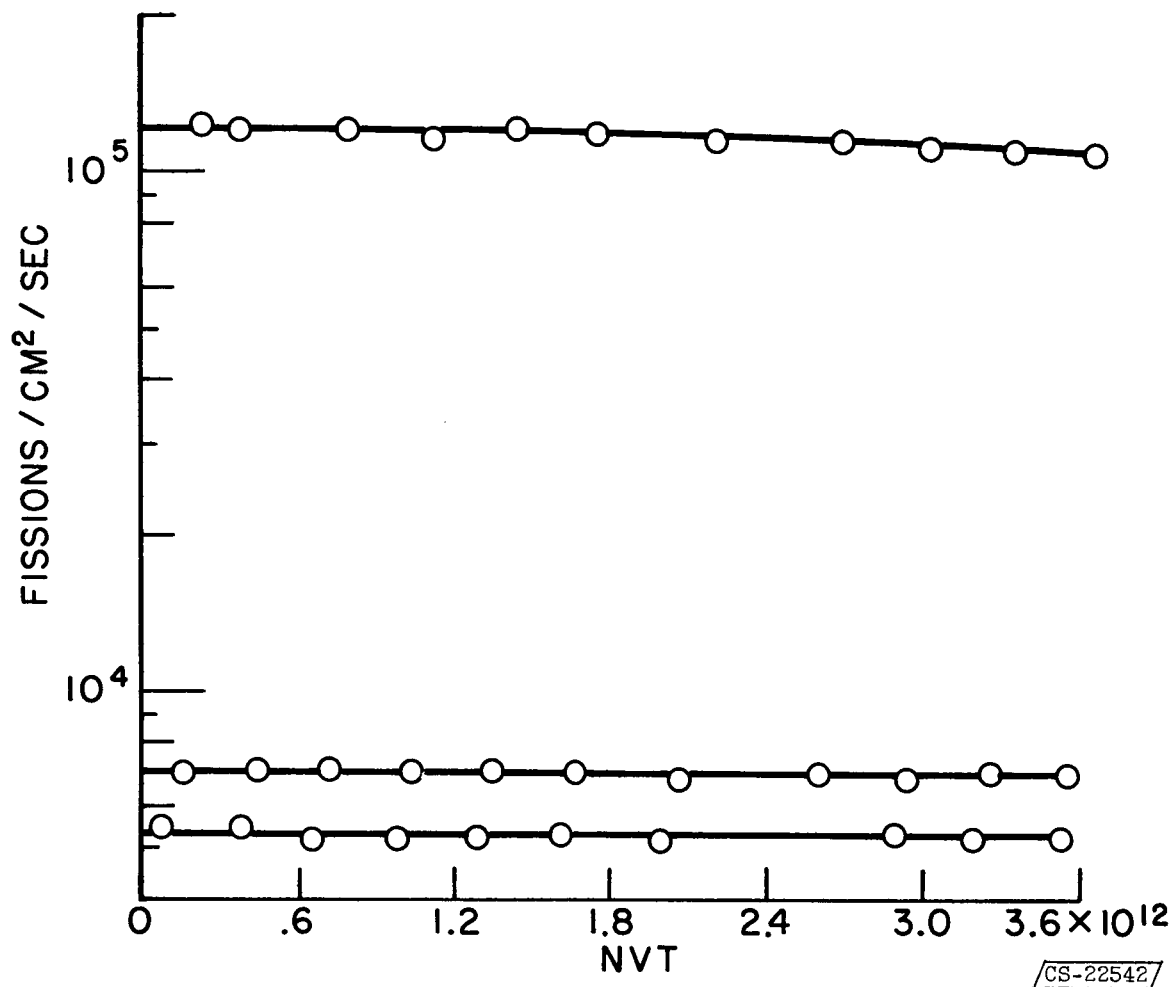


Figure 10. - Count rate as a function of integrated thermal flux for three detectors, each with a different thickness of uranium-235 on its surface.

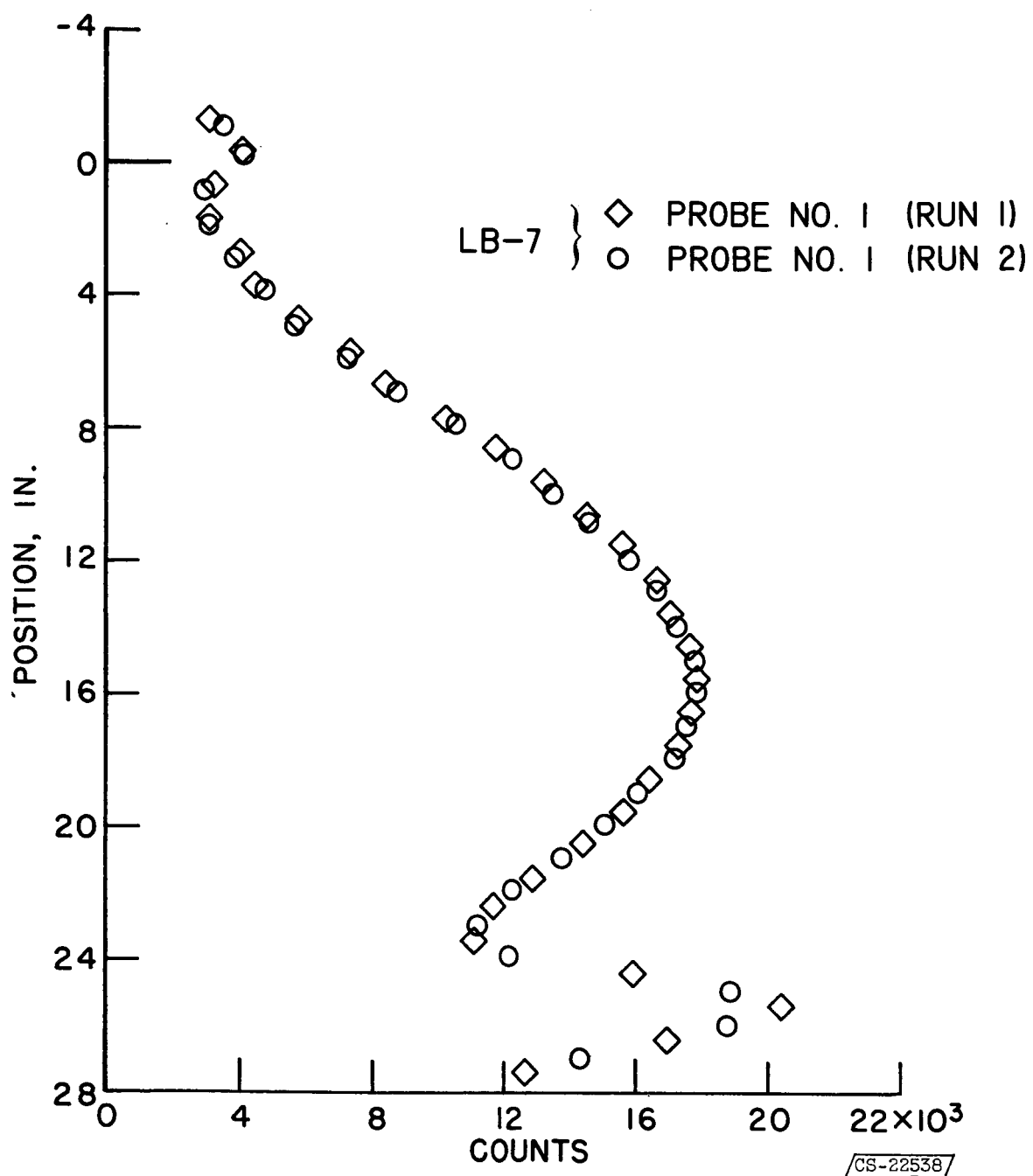


Figure 11. - Vertical flux traverse in LB-7 (run No. 1) with repeat (run No. 2) after mapping 10 elements.

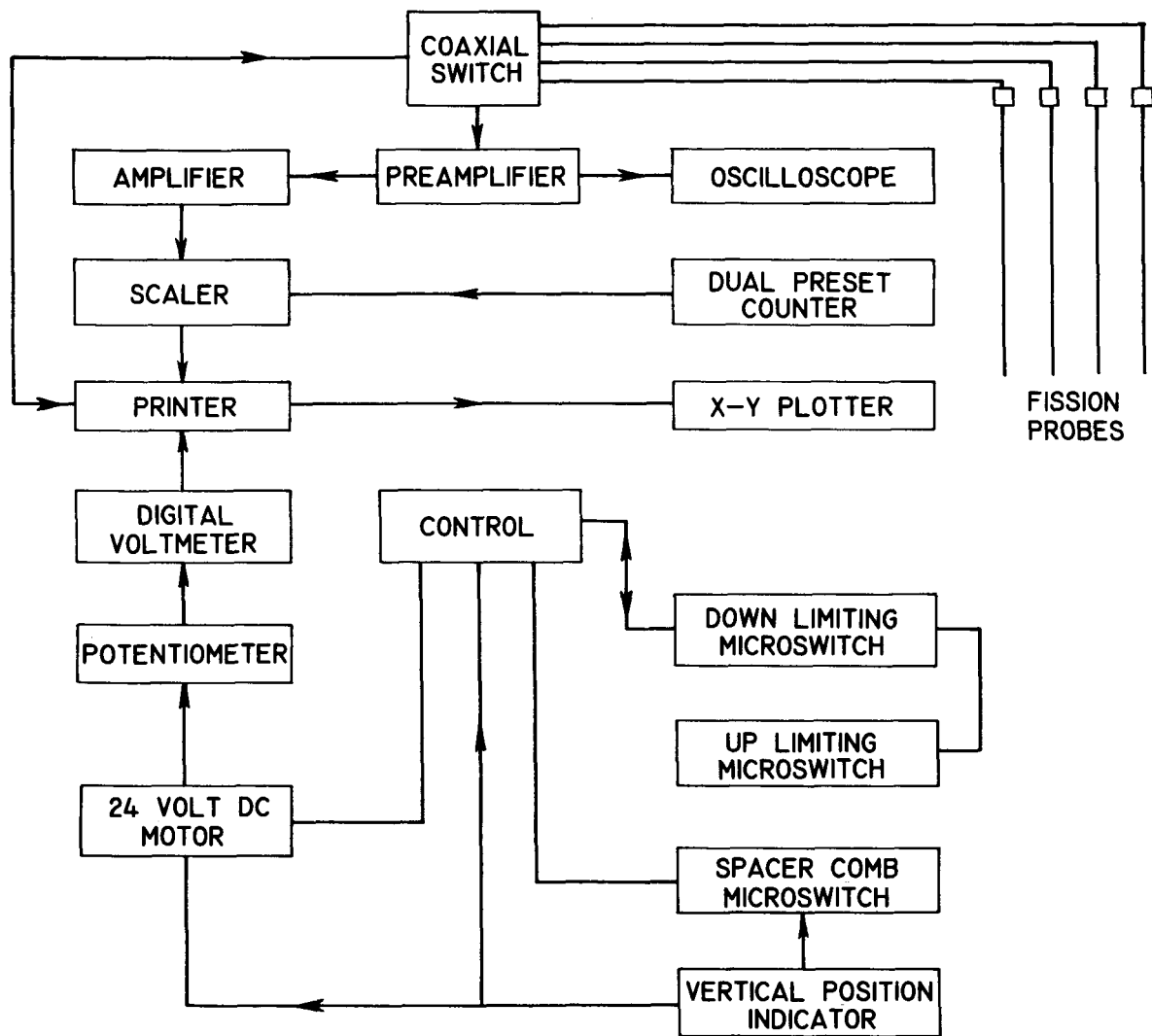


Figure 12. - Block diagram of control instrumentation and readout equipment.

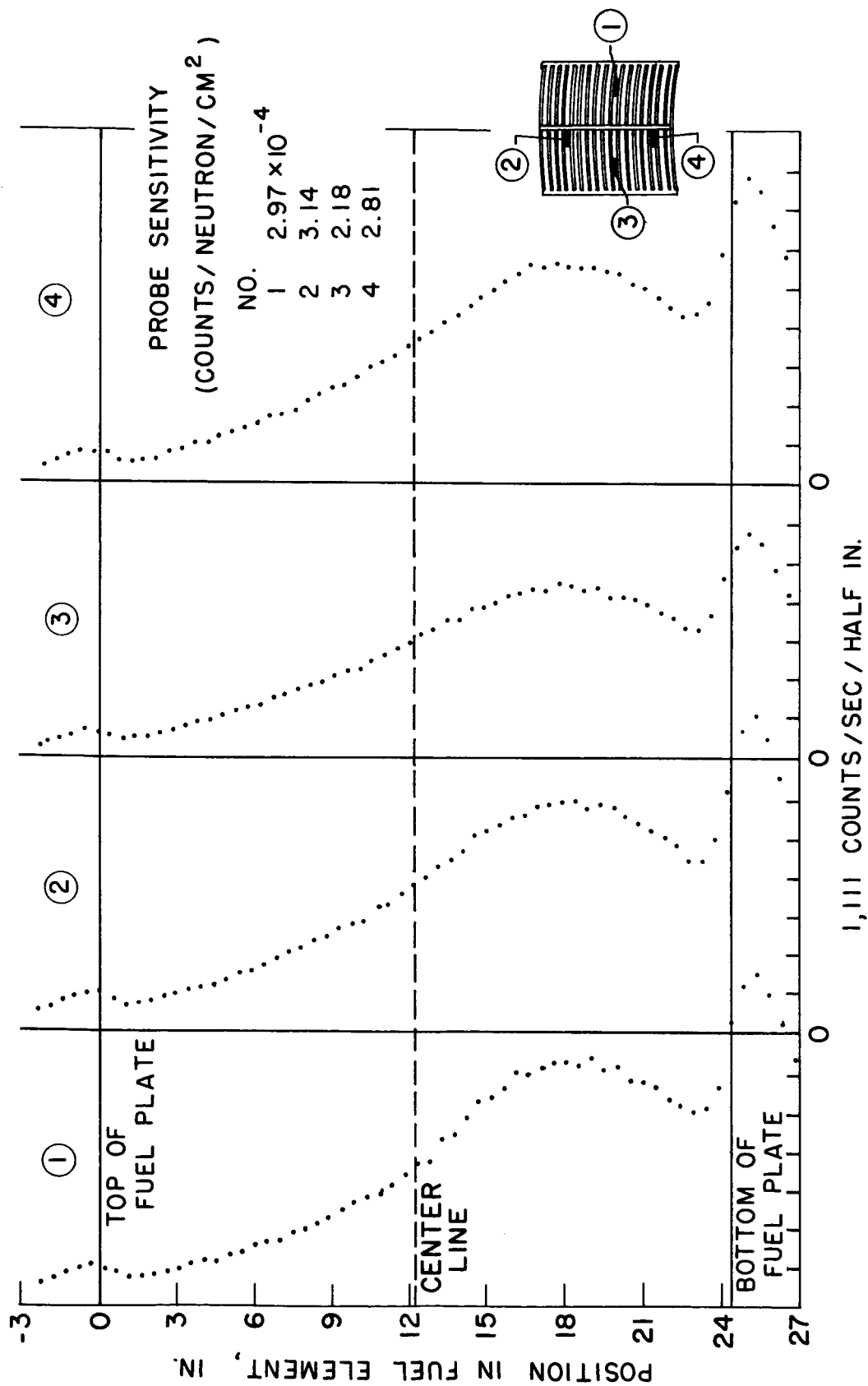


Figure 13. - Typical set of flux data made by the x-y plotter during a traverse.

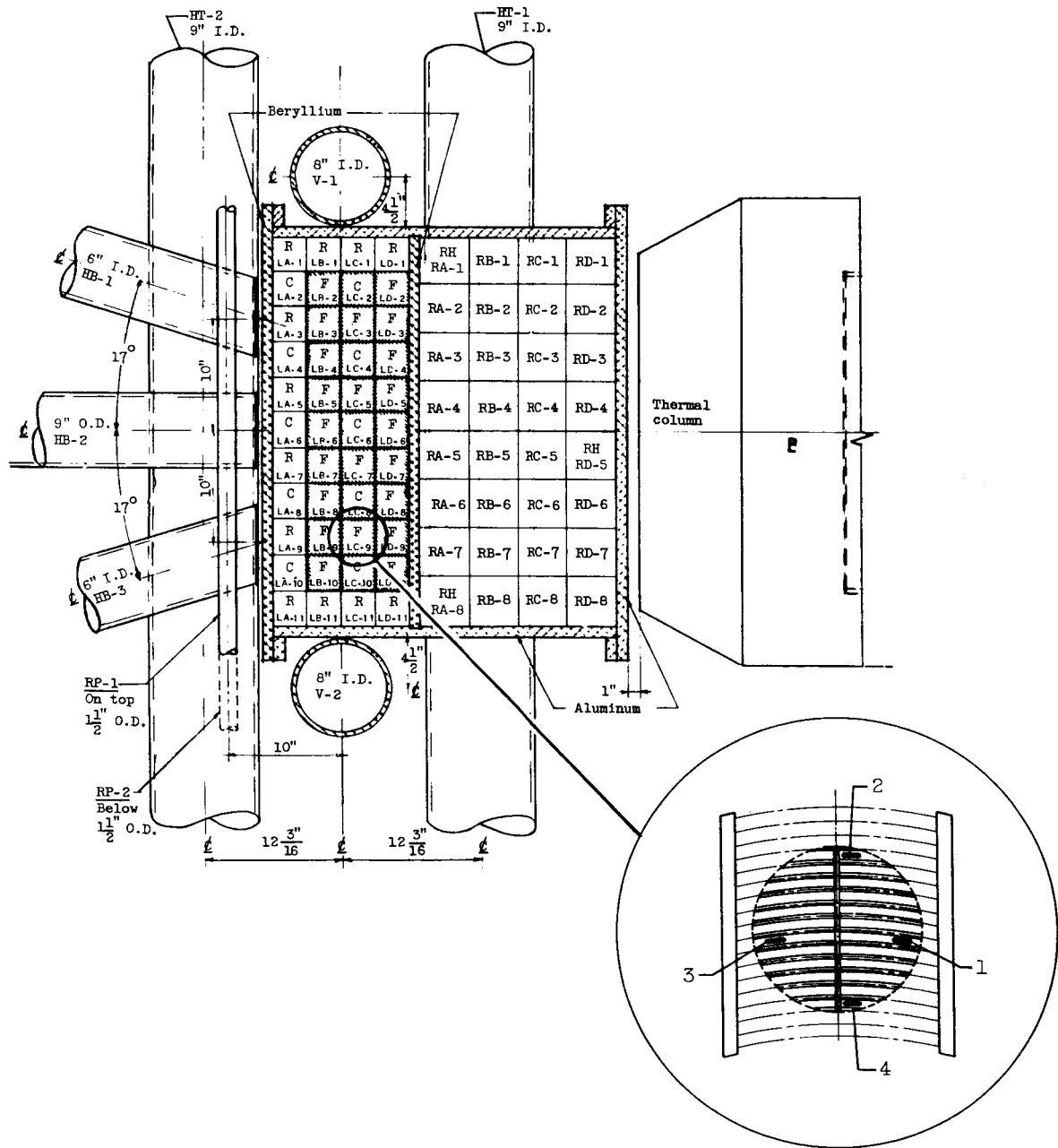


Figure 14. - Plan view of PBR.

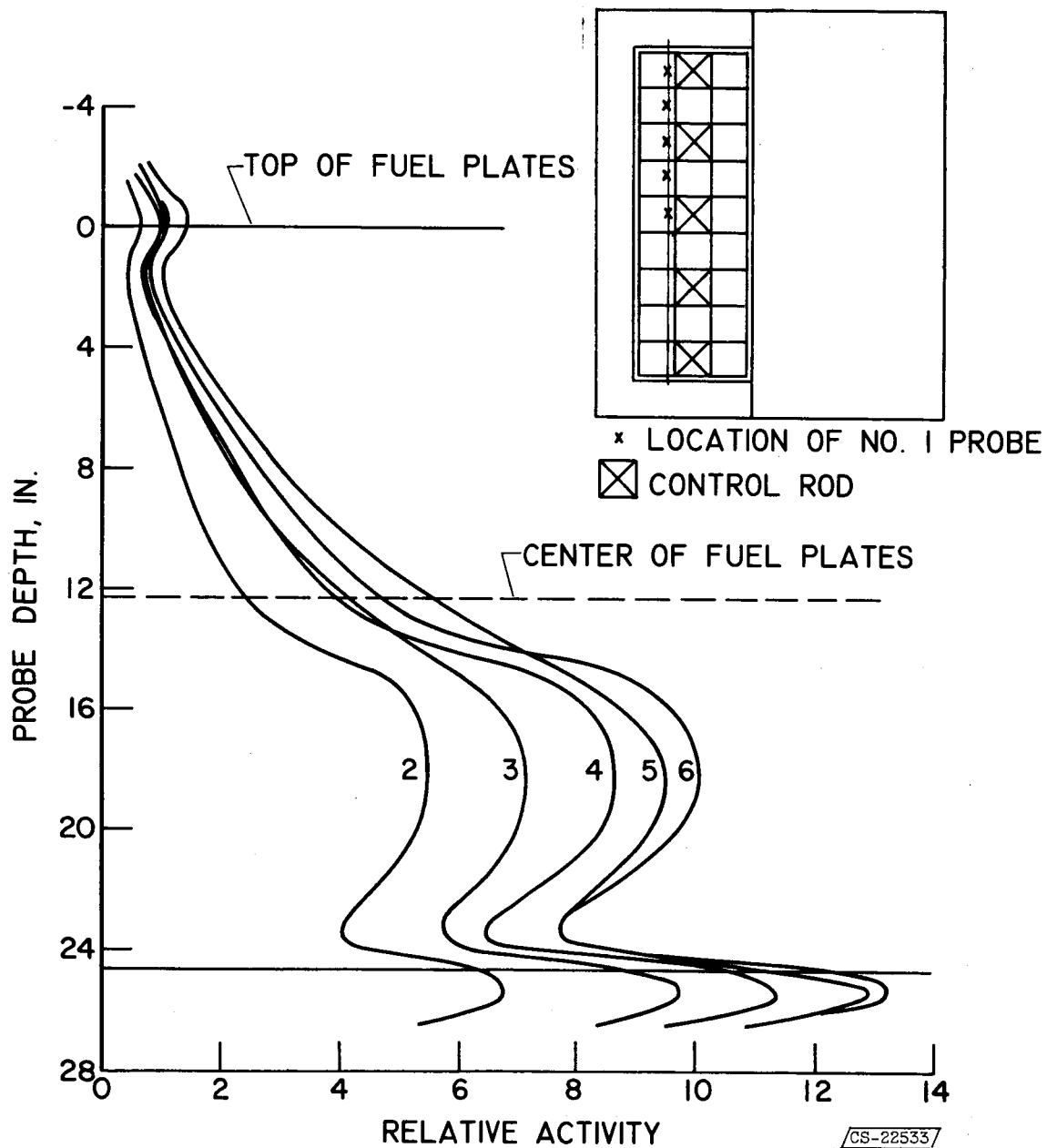


Figure 15. - Family of vertical flux traverses made with probe No. 1 in elements LB-2, LB-3, LB-4, LB-5, and LB-6.

CS-22533



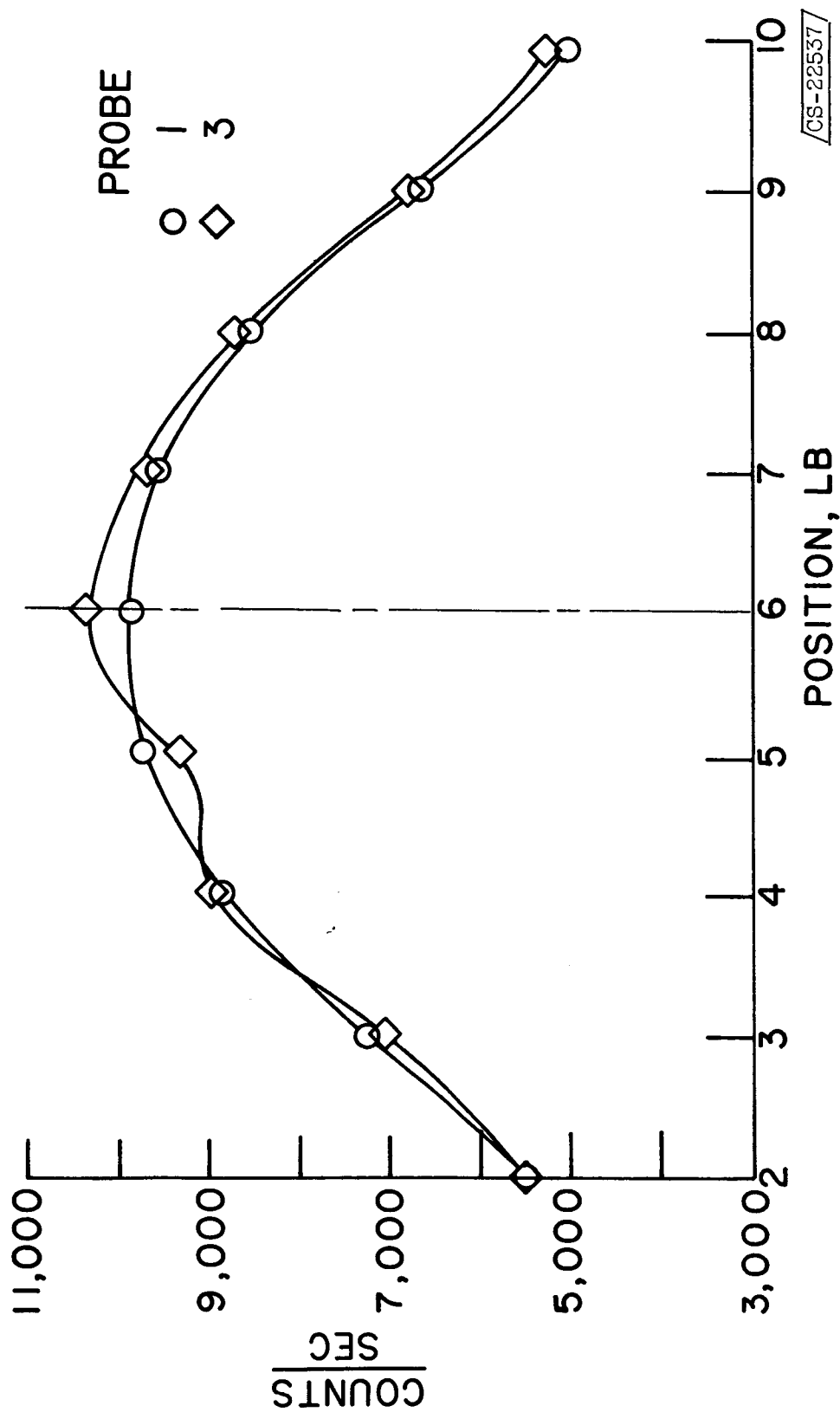
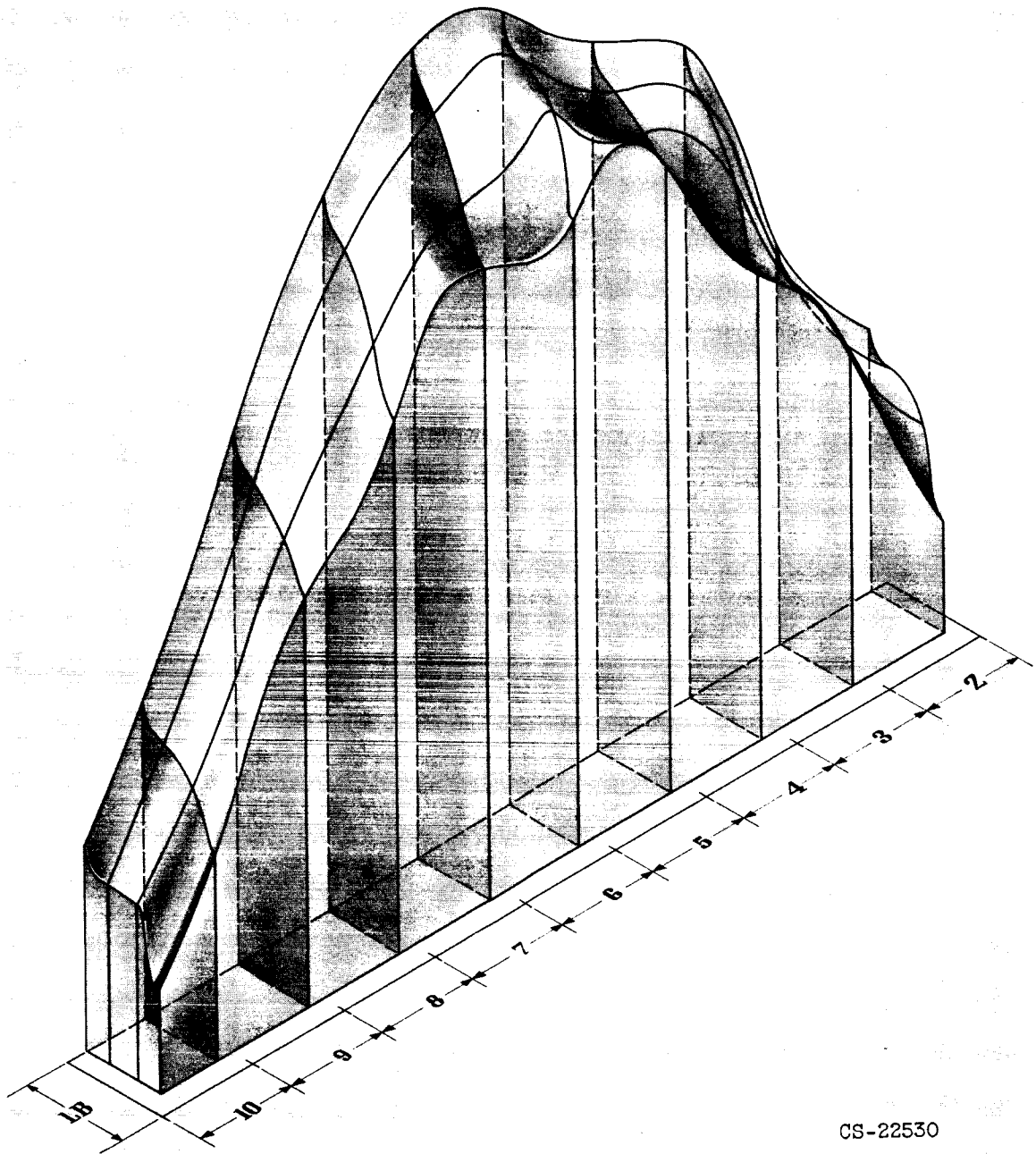
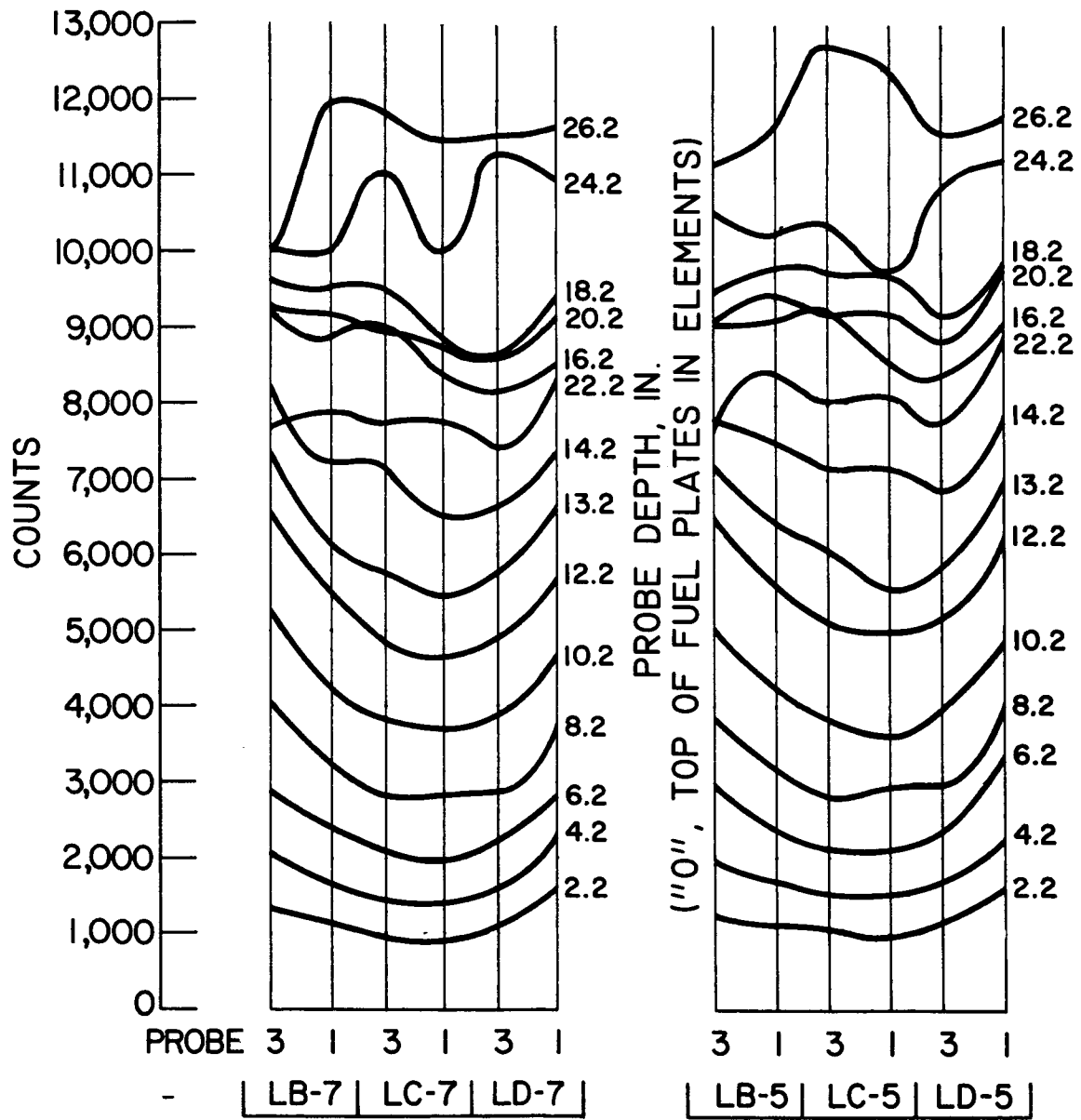


Figure 16. - Horizontal traverse constructed across LB row at 18.7 inches.



CS-22530

Figure 17. - Three dimensional flux distribution generated from traverses in LB row.



CS-22536/

Figure 18. - Family of horizontal traverses across LB-5, LC-5, LD-5, and also LB-7, LC-7, LD-7.

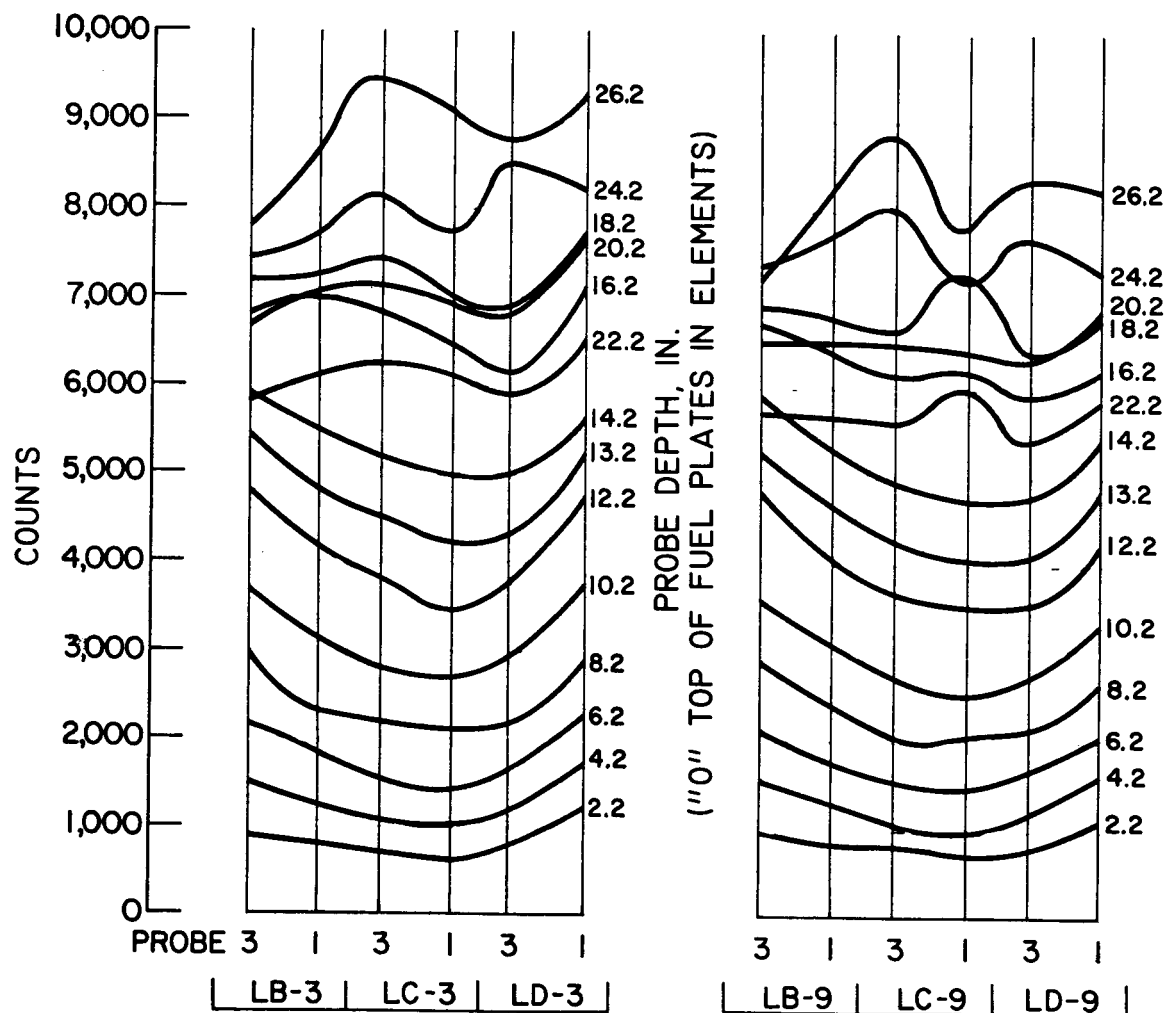


Figure 19. - Family of horizontal traverses across LB-3, LC-3, LD-3, and also LB-9, LC-9, LD-9.

CS-22535